JOETSR-International Journal of Emerging Trends in Scientific Research
Special Issue Volume 1, Issue 1 | December-2025
e-ISSN: 2997-8718 Print ISSN: 2997-870X

A Novel DISB Converter to Facilitate Multi Functions in EV Applications

Alli Raja[1], Arpula Krishnaiah[2], Maisakhsi Pavan kumar[3]
[1]Electrical and Electronics Engineering & KLR Engineering College, Palvancha Telangana
[2]Electrical and Electronics Engineering & KLR Engineering College, Palvancha Telangana
[3]Electrical and Electronics Engineering & KLR Engineering College, Palvancha Telangana
Received: 07-10-2025; Revised: 14-11-2025; Accepted: 24-11-2025; Published: 08-12-2025

Abstract
One more renewable electricity technology that gains more and more significance is offshore wind power, which is motivated by the necessity to decrease the levelized cost of energy by using the multi-megawatt wind turbines and power conversion systems that provide high performance, high power density, and high reliability. One way out is an alternative to traditional electromechanical energy conversion architectures, where a multi-port permanent magnet synchronous generator is coupled to one active rectifier (up to) and many passive rectifiers.In offshore wind market, it is crucial to have an effective maximum power point tracking (MPPT), but effectively implementing MPPT in those kind of integrated systems is very difficult, as passive rectifiers cannot be controlled directly. As illustrated in this paper, it can be established that efficient MPPT can still be achieved by taking advantage of the fact that the d-axis current of the active rectifier can be used to control the overall output power of the system. The proposed scheme provides a substantial boost to the viability and possibility of integrated power conversion systems to be utilized in offshore wind energy derivatives, by allowing the utilization of reliable MPPT.

Keywords: ***Multi-port converter, electric vehicle, bidirectional dc/dc converter, battery storage, Regenerative charging.***

1.Introduction
Transportation that uses electric motors has experienced a massive popularity over the past decades owing to the environmental effects of transport systems that utilize petroleum. In comparison to traditional cars, electric vehicles (EVs) use electric energy which can be produced by a broad variety of sources, such as fossil fuels, renewable energy resources, and nuclear power. Different models of storage include batteries or supercapacitors to store this electrical energy. Therefore, the rising popularity of EVs has resulted in more studies on energy storage systems, bidirectional DC-DC converters, and uninterruptible power supplies(1).

Conventionally, the bidirectional power conversion has been very popular with the dual active bridge (DAB) converter. The DAB converter however has difficulty in attaining zero-voltage switching (ZVS) with large swings in the input and output voltage. To overcome this shortcoming, the phase-shift control and pulse-width modulation (PWM) methods have been implemented into the control plan. Also, bidirectional DCDC conversion has been achieved with a voltagefed inverter on the high voltage side of a transformer and a currentfed inverter on the low voltage side. With these advances conventional converter topologies continue to experience high switching losses, and are not easily able to sustain ZVS in the presence of large load variations. To address these negative aspects, a resonant-induced bidirectional DC-DC converter is suggested, which can minimize the losses of switching and enhance the overall performance of the converter to a large extent.

Emerging technologies of the vehicles have been brought about due to the growing environmental pollution, depletion of fossil fuel resources, global warming and escalating fuel prices. Due to this, the automotive industry has been keen on the design of the hybrid electric vehicles (HEVs) and the electric vehicles that are friendly to the environment. Another important element of these cars is the motor drive system, which has to be fueled by an effective power electronic converter. In EVs, such a converter has to allow a two-directional flow of power between the energy sources, batteries, and motor drive systems(2).

Many works have been documented in the literature on power electronic interfaces concerning EV systems. Types of non-isolated three-port converter topology, based on a dual-input converter (DIC), a dual-output converter (DOC), and a single-input single-output (SISO) converter are described in [1]. In [2], high step-up DC2DC converter that incorporates the attributes of buck-boost converter and KY converter is proposed in order to attain the high voltage conversion ratio(3).

2. Proposed System

The main input of this paper is to suggest a single-phase, transformerless four-port bidirectional buck-boost converter (FPC) which uses three switches only. The proposed converter has a number of benefits over other topologies, which have been described in the literature (see Table 1) such as a modular design, fewer components and the capability of connecting a multiplicity of input sources with varying voltagecurrent characteristics(4). The converter can also generate an output voltage which is larger than the maximum input voltage (boost mode) or smaller than the minimum input voltage (buck mode). Maximum switching losses are minimized to increase converter efficiency.

Since the input power and the condition of dynamic loads in EV systems vary, in most cases a single energy source is not adequate to sustain the load demands. Hence there is need to hybridize several energy sources. The primary aim of the work is the creation of converter topology that would be able to bridge a vehicle drive train and various energy sources. Figure 1(a) and 1(b) depict the position of the power electronic interface in an EV power system whereas Figure 2 demonstrates the four-port converter topology that is proposed.

The salient key characteristics of the proposed converter are that the flow of power between the load and input sources is controlled by three actively controlled switches, Q1, Q2, and Q3 as shown in Figure 2. Five different modes are used in a converter and they are as shown in Figures 3(a) 3(e). State 1 is the operation of a single-Input dual-Output (SIDO) model: the EV drives are fed by photovoltaic (PV) energy (Figure 3a). The charge to the battery may be taken off the PV source or off the load as illustrated in Figures 3(b) and 3(e). The State 5 is the state in which the battery receives power from the load in regenerative braking(5). In situations where the solar irradiation is low and the PV source is unable to generate enough power to meet the load demand the battery is discharged to satisfy the load demand (Figure 3c). At high power demand times, the battery and PV source collaborate to provide energy to the drivetrain, and it operates in a dual-input dual-output (DIDO) mode (Figure 3d). Figures 4 and 5 show the switching schemes and equivalent circuit of the switching at various conditions of operation.

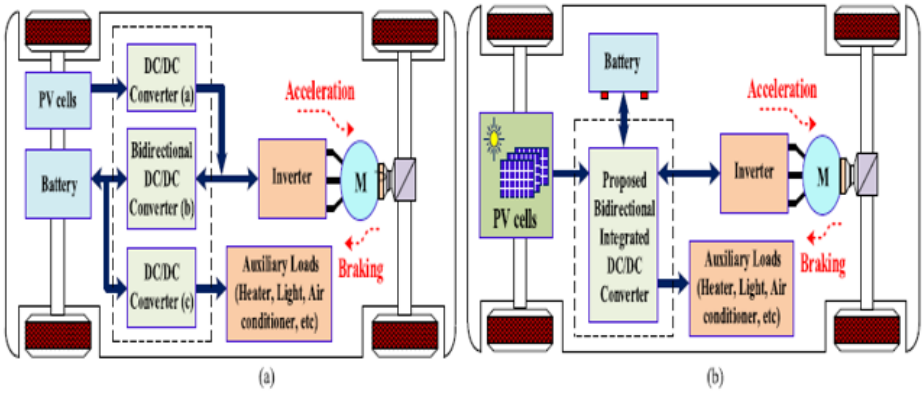

FIGURE 1 Block Diagram of conventional converter proposed Integrated four-port converter (FPC) inferface in an electric vehicle system

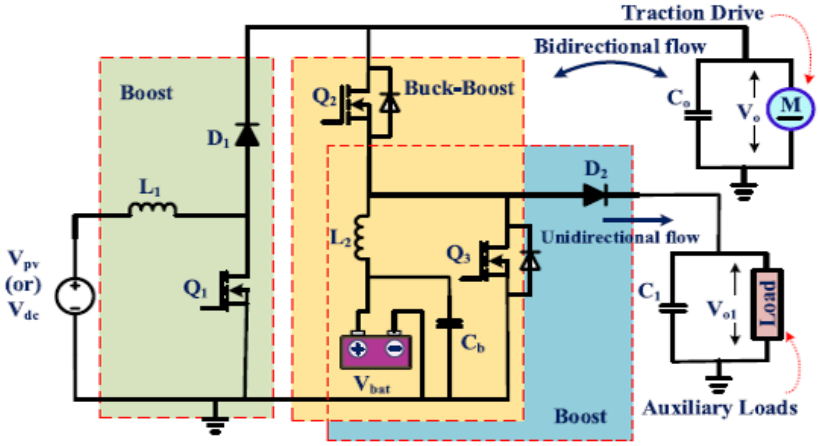

FIGURE 2 Topology Diagram of four-port (FPC) Converter

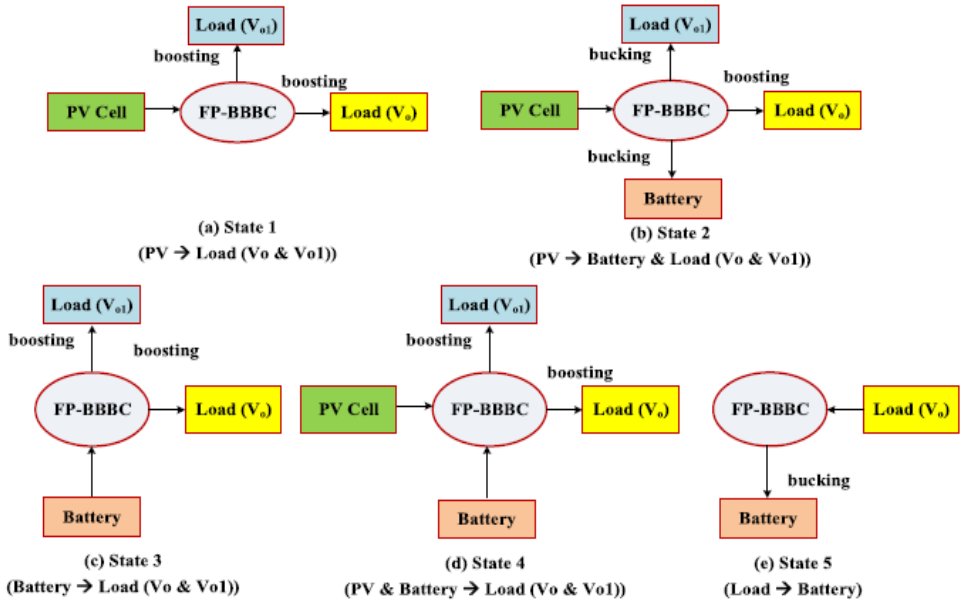

FIGURE 3 a)State 1(boost), State 2 (buck & boost), c)State 3 (boost), d)State 4(boost), e)State

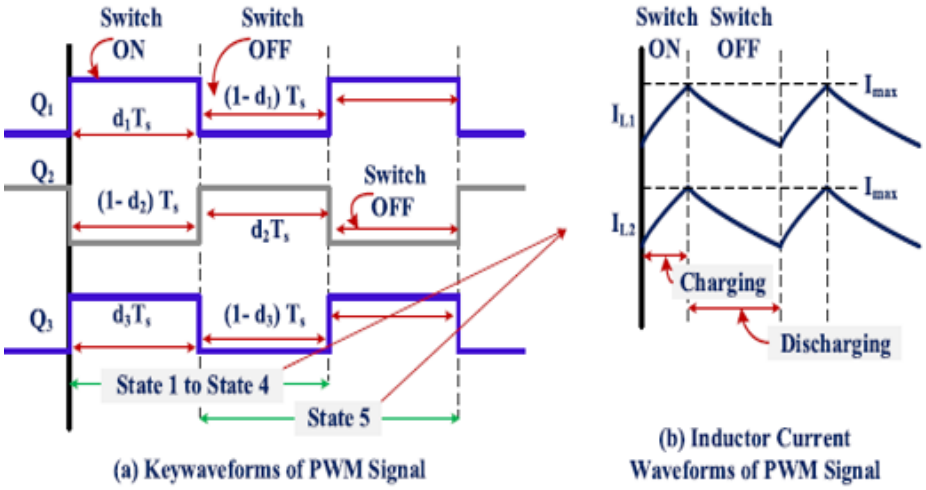

FIGURE 4 State of operation proposed FPC

3.Operating Modes- State of Operation

State 1: PV-to-Load Power Transfer

In this operating state, the photovoltaic (PV) source independently supplies power to the load. The corresponding switching states of the converter are summarized in Table 2. During the interval 0≤t≤d1Ts0 \leq t \leq d_1T_s0≤t≤d1Ts, switches Q1Q_1Q1 and Q3Q_3Q3 are turned ON, while Q2Q_2Q2 remains OFF(6). Assuming Vpv>VbatV_{pv} > V_{bat}Vpv>Vbat (see Figures 5(a) and 5(b)), the PV voltage appears across inductor L1L_1L1, causing the inductor current to increase linearly with a positive slope(7).

During the interval d1Ts≤t≤Tsd_1T_s \leq t \leq T_sd1Ts≤t≤Ts, switches Q1Q_1Q1 and Q3Q_3Q3 are turned OFF and Q2Q_2Q2 is turned ON. The energy stored in inductor L1L_1L1 during the previous interval is then transferred to the output capacitor through diode D1D_1D1. Here, TsT_sTs denotes the switching period.

$$V_o = \frac{1}{1-d_1} V_{pv} \qquad (3)$$

$$V_{o1} = d_2 V_{pv} \qquad (4)$$

$$V_{bat} = d_2 V_{pv} \qquad (5)$$

State 2: PV-to-Battery Charging and Load Boosting

This state operates in a manner similar to State 1. When the battery requires charging from the PV source, switch Q2Q_2Q2 is controlled with a duty ratio d2<0.5d_2 < 0.5d2<0.5, as shown in Figures 5(c) and 5(d). For d1>0.5d_1 > 0.5d1>0.5, switch Q3Q_3Q3 operates in a manner analogous to Q1Q_1Q1 to provide a boosted output voltage across the load. The relationship between the PV voltage (VpvV_{pv}Vpv), battery voltage (VbatV_{bat}Vbat), and output voltages (VoV_oVo, Vo1V_{o1}Vo1) can be derived accordingly.

$$V_o = \frac{1}{1-d_3} V_{bat} \qquad (6)$$

$$V_{o1} = \frac{1}{1-d_3} V_{bat} \qquad (7)$$

TABLE 1 State of Operation

No.of States	Input Sources	MOSFET Switches			Inductors		Diodes		Battery	Capacitors		Outputs	
		Q_1	Q_2	Q_3	L_1	L_2	D_1	D_2	V_{bat} (or) C_b	C_o	C_1	(V_o)	(V_{o1})
State 1 (V_{pv}>V_{bat})	(V_{pv}) or (V_{dc})	ON	OFF	ON	↑	↑	OFF	OFF	-	↓	↓	Boost	Boost
		OFF	ON	OFF	↓	↓	ON	ON		↑	↑		
State 2 (V_{pv}>V_{bat})	(V_{pv}) or (V_{dc})	ON	OFF	ON	↑	↓	OFF	OFF	↑	↓	↓	Boost	Boost
		OFF	ON	OFF	↓	↑	ON	ON		↑	↑		
State 3 (V_{pv}<V_{bat})	(V_{bat})	-	OFF	ON	-	↑	-	OFF	↓	↓	↓	Boost	Boost
		-	ON	OFF	-	↓	-	ON		↑	↑		
State 4 (V_{pv}=V_{bat})	(V_{pv}) and (V_{bat})	ON	OFF	ON	↑	↑	OFF	OFF	↓	↓	↓	Boost	Boost
		OFF	ON	OFF	↓	↓	ON	ON		↑	↑		
State 5 (V_{pv}=0, V_{bat}<V_{load})	Regenerative braking power	-	ON	OFF	-	↑	-	ON	↑	↓	↓	Buck	Buck
		-	OFF	ON	-	↓	-	OFF		↑	↑		

Table representation: **ON**- Switch close, **OFF**- Switch open, ↑- charging of inductor and capacitor, and ↓- discharge of inductor and capacitor

State 3: Battery-to-Load Power Transfer

In this mode, the load is supplied solely by the battery. During battery discharge, the inductor current iL2i_{L2}iL2 increases linearly in the interval 0≤t≤d3Ts0 \leq t \leq d_3T_s0≤t≤d3Ts. Between d3Tsd_3T_sd3Ts and TsT_sTs , the inductor current decreases with a negative slope. Switch Q3Q_3Q3 is actively controlled to boost the drivetrain output voltage, while switch Q1Q_1Q1 remains OFF since it does not participate in energy transfer from the battery to the load (see Figures 5(e) and 5(f)). The resulting output voltage across the load during battery discharge can be expressed accordingly(8).

$$V_o = \frac{1}{1-d_1} V_{pv}, \text{ (or) } V_o = \frac{1}{1-d_3} V_{bat} \qquad (8)$$

$$V_{o1} = \frac{1}{1-d_1} V_{pv}, \text{ (or) } V_{o1} = \frac{1}{1-d_3} V_{bat} \qquad (9)$$

State 4: Combined PV and Battery Power Supply (High Power Demand)

When the EV experiences high power demand, both the PV source and the battery simultaneously supply energy to the drivetrain, as illustrated in Figures 4(a) and 4(b). During the interval 0≤t≤d1Ts0 \leq t \leq d_1T_s0≤t≤d1Ts , switches Q1Q_1Q1 and Q3Q_3Q3 are gated ON, charging inductors L1L_1L1 and L2L_2L2, and causing currents iL1i_{L1}iL1 and iL2i_{L2}iL2 to increase linearly. At the same time, a complementary gating signal is applied to switch Q2Q_2Q2(9).

When switches Q1Q_1Q1 and Q3Q_3Q3 are turned OFF, the inductor currents decrease with a negative slope, and diodes D1D_1D1 and D2D_2D2 conduct, delivering energy from both the PV source and the battery to the load. The net output voltage resulting from the combined power contribution of both sources can be calculated using Equations (8) and (9).

$$V_{bat} = d_2 V_o \qquad (10)$$

$$V_{O1} = d_3 V_o \qquad (11)$$

State 5: Regenerative Braking Mode

During regenerative braking, the kinetic energy stored in the drivetrain is converted into electrical energy and transferred back to the battery, as shown in Figures 5(i) and 5(j). In this state, switch Q2Q_2Q2 is turned OFF, switch Q3Q_3Q3 is turned ON, and switch Q1Q_1Q1 remains OFF throughout the operation. The battery is charged through the coordinated ON/OFF operation of switches Q2Q_2Q2 and Q3Q_3Q3. Simultaneously, regenerative braking energy supports the second output, thereby reducing battery stress. The corresponding control relationship for this operating mode can be derived accordingly.

4. Fault Analysis of the Converter

An analysis of converter operation under fault conditions is summarized as follows:

Case 1: If switch Q1Q_1Q1 fails in the open state, diode D1D_1D1 becomes reverse-biased, preventing the transfer of increased PV power. In this scenario, the converter continues to supply power to the load using the available battery energy while operating in single-input multiple-output (SIMO) mode. Switches Q2Q_2Q2 and Q3Q_3Q3 can still charge the battery using any available regenerative braking energy(10).

Case 2: If switch Q2Q_2Q2 fails open, the PV source cannot charge the battery, and auxiliary loads cannot be supplied during regenerative braking. However, the converter continues to operate in single-input single-output (SISO) mode, allowing the PV source to supply power directly to the traction drive.

Case 3: If switch Q3Q_3Q3 fails open, both charging and discharging operations of the battery are affected. Consequently, the battery is unable to provide boosted output voltage under varying load conditions.

Case 4: Switch Q1Q_1Q1 normally provides a boosted output voltage to the load through diode D1D_1D1 during its ON–OFF switching action. If diode D1D_1D1 fails open, the load will not receive boosted output voltage, and current will circulate through the switch and inductor L1L_1L1, potentially leading to excessive heating. Similarly, if diode D2D_2D2 fails open, power transfer to the load through that path will be completely interrupted.

4. Simulation Results

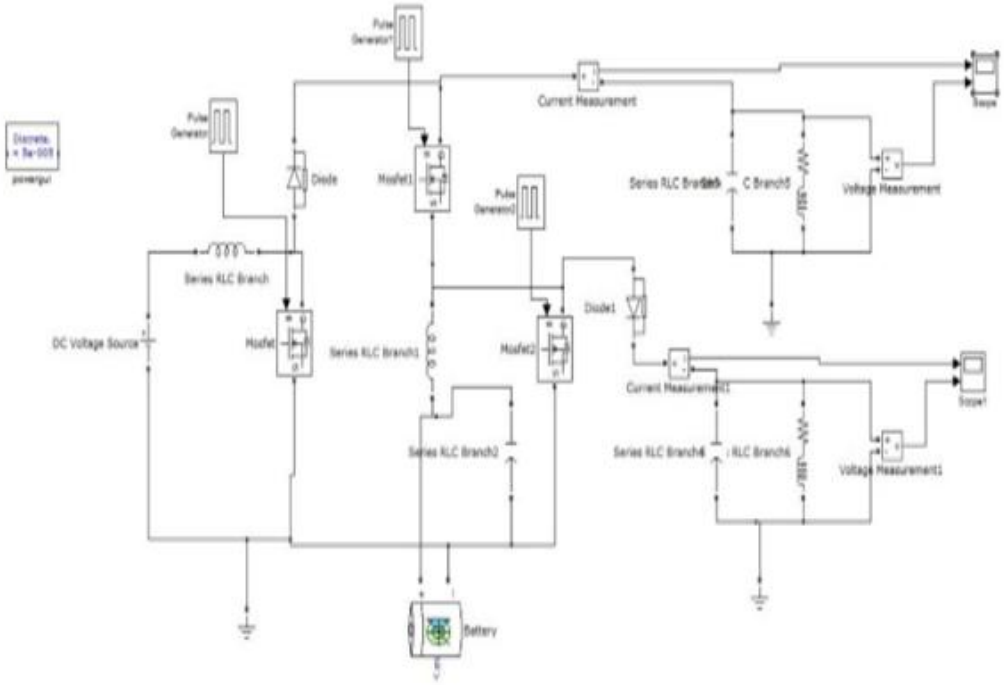

FIGURE 6 Simulation of Open Motor Loop

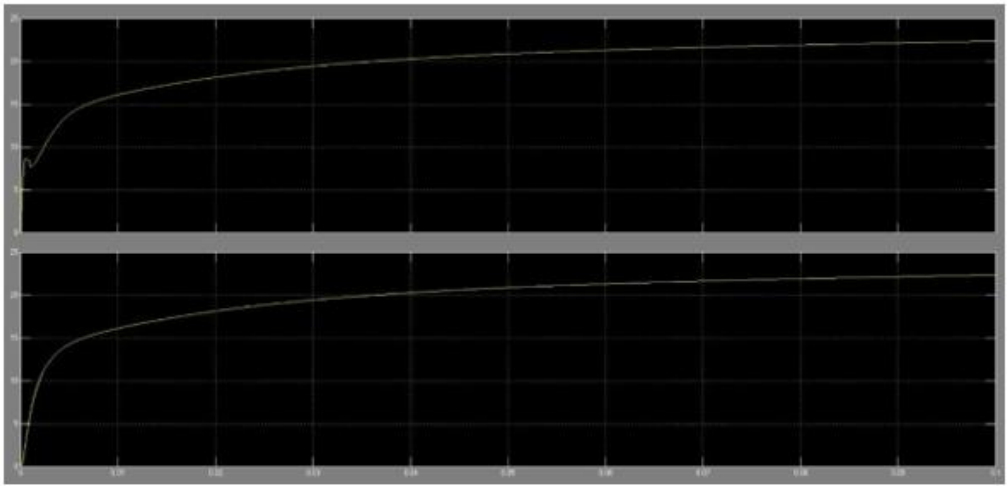

FIGURE 7 Output of Open Motor Loop

4.1 Simulation Circuits of Motor Closed Loop With Control

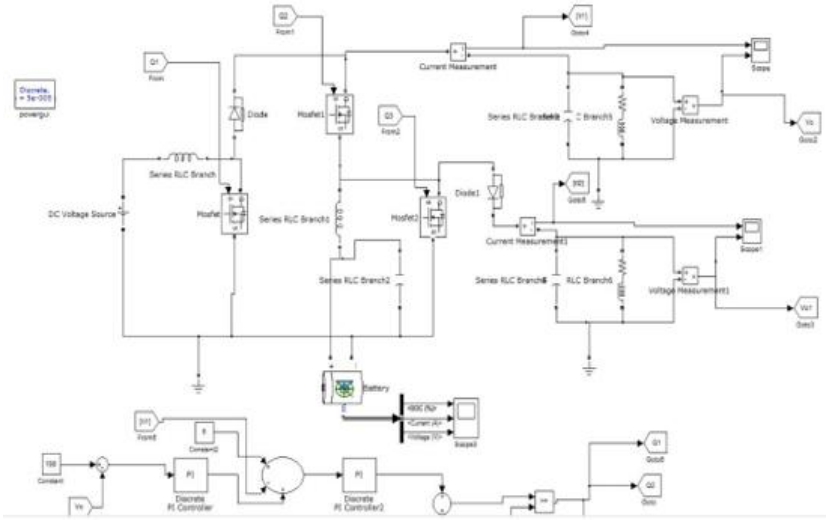

FIGURE 8 Simulation of Closed Loop

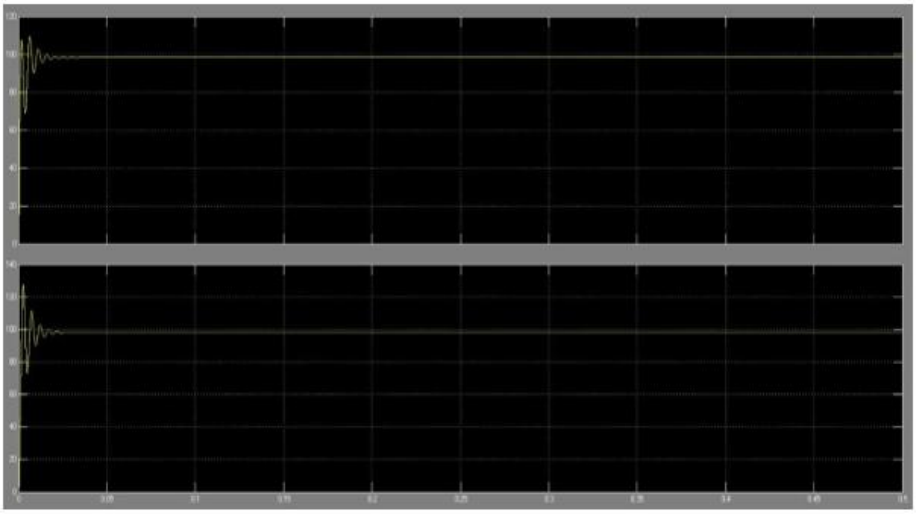

FIGURE 9 Output of Closed Loop

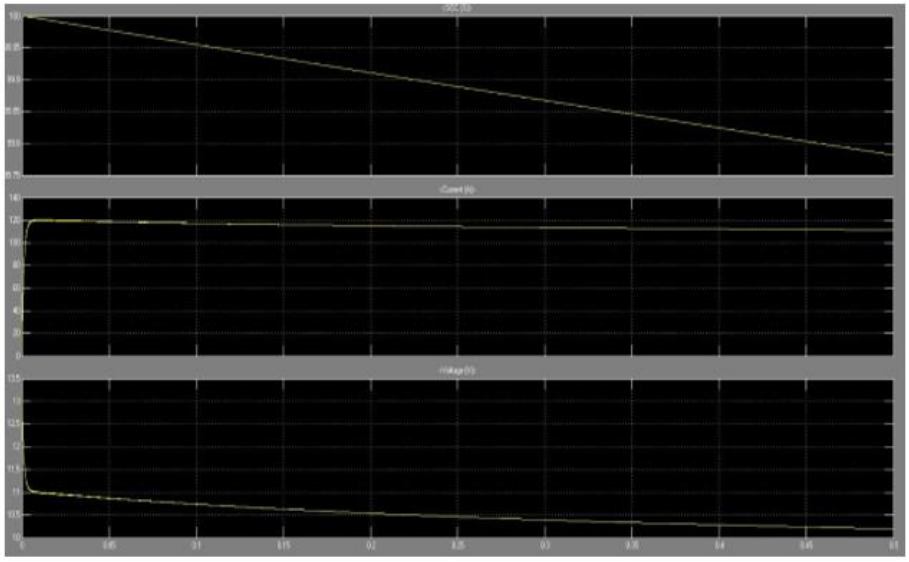

FIGURE 10 Battery Parameters of Closed Loop

5. Conclusion

This study is a proposal about a single-stage four-port buck-boost converter to hybridize various energy streams to electric vehicle. The improvements of this converter over the existing buck-boost converter topologies in the literature include: a) it can generate both buck, boost and buck-boost output with no extra transformer required, b) it can support multiple resources with different voltage and current capacity and c) the converter has the capability of a two-way power flow with fewer components. The mathematical analysis has shown the functions of the proposed converter. A simple control technique has been used to budget the power flow between the input sources. Finally, the functionality of the converter has been confirmed with the help of a low voltage prototype model. The feasibility of the proposed four-port buck-boost topology using the results of the simulation..

Acknowledgement: Nil

Conflicts of interest

The authors have no conflicts of interest to declare

References

1. Wu H, Xing Y, Xia Y, Sun K. A family of non-isolated three-port converters for stand-alone renewable power systems. IEEE Transactions on Power Electronics. 2011;1(11):1030–1035.
2. Hwu KI, Huang KW, Tu WC. Step-up converter combining KY and buck–boost converters. Electronics Letters. 2011;47(12):722–724.
3. Xiao H, Xie S. Interleaving double-switch buck–boost converter. IET Power Electronics. 2012;5(6):899–908.
4. Kang H, Cha H. A new non-isolated high-voltage-gain boost converter with inherent output voltage balancing. IEEE Transactions on Industrial Electronics. 2018;65(3):2189–2198.
5. Bang T, Park JW. Development of a ZVT-PWM buck cascaded buck–boost PFC converter of 2 kW with the widest range of input voltage. IEEE Transactions on Industrial Electronics. 2018;65(3):2090–2099.
6. Lin CC, Yang LS, Wu GW. Study of a non-isolated bidirectional DC–DC converter. IET Power Electronics. 2013;6(1):30–37.
7. Khan MA, Ahmed A, Husain I, Sozer Y, Badawy M. Performance analysis of bidirectional DC–DC converters for electric vehicles. IEEE Transactions on Industry Applications. 2015;51(4):3442–3452.
8. Dusmez S, Khaligh A, Hasanzadeh A. A zero-voltage-transition bidirectional DC/DC converter. IEEE Transactions on Industrial Electronics. 2015;62(5):3152–3162.
9. Zhu H, Zhang D, Zhang B, Zhou Z. A non-isolated three-port DC–DC converter and three-domain control method for PV–battery power systems. IEEE Transactions on Industrial Electronics. 2015;62(8):4937–4947.
10. Camara MB, Gualous H, Gustin F, Berthon A. Design and new control of DC/DC converters to share energy between supercapacitors and batteries in hybrid vehicles. IEEE Transactions on Vehicular Technology. 2008;57(5):2721–2735.